

## Structure and in Vitro Digestibility of Normal Corn Starch: Effect of Acid Treatment, Autoclaving, and $\beta$ -Amylolysis

WEI SONG, SRINIVAS JANASWAMY, AND YUAN YAO\*

Department of Food Science, Purdue University, 745 Agriculture Mall Drive, West Lafayette, Indiana 47907-2009

The goal of this study was to explore a new strategy to reduce the digestibility of normal corn starch (NCS). NCS was treated using 1.0% hydrogen chloride at 55 °C. After neutralization and desalting, starches were adjusted to 35% moisture content and subjected to autoclaving. Thereafter, starches were subjected to  $\beta$ -amylolysis. At different stages, starches were characterized for chain length distribution, ordered structure including the crystalline pattern, and in vitro digestibility. The results showed that acid treatment reduced amylose molecular weight and increased the thermal resistance of A-type crystallites. V-type crystallites promoted by autoclaving were increased by acid treatment, suggesting the beneficial effect of reduced amylose molecular weight on crystallization.  $\beta$ -Amylolysis had minor impact on the crystalline pattern; however, it significantly reduced the in vitro digestibility of starch by enriching linear chains. At higher levels of acid treatment, the effect of  $\beta$ -amylolysis was more pronounced.

**KEYWORDS:** Starch digestibility; acid treatment; autoclaving;  $\beta$ -amylolysis

### INTRODUCTION

Controlled digestibility of starch-containing foods may help to address a number of health issues, specifically those related to glucose absorption, glycemic index, and colon health. In the past, significant works have been accomplished to modulate starch digestibility, for example, by increasing the amount of resistant starch in food. Resistant starch has been understood as the starch component that avoids amylolysis in the small intestine and enters the colon for fermentation. According to Englyst et al. (1), by their digestion behaviors, starch materials can be classified into rapidly digestible starch (RDS), slowly digestible starch (SDS), and resistant starch (RS). The properties of various RS types and approaches for preparing them have been extensively discussed (2).

Due to their capability to form stable crystallites, long linear  $\alpha$ -glucans such as amylose are favored for preparing RS. High-amylose corn starch (HACS), which may contain up to 70% amylose, is the most preferred starting material for preparing RS-containing food ingredients (2). Starches with lower amylose content have also been utilized for this purpose, mostly through enzymatic debranching to generate linear glucans (3–5). Debranching releases linear chains from amylopectin to promote the formation of ordered structure. However, compared with HACS, materials prepared by debranching low-amylose starch contain short chains as the primary components, limiting the formation or stability of double helices and crystallites (6). The study by Eerlingen et al. (7) showed that the chain length of RS ranges from DP19 to DP26 and is independent of amylose chain length

and that the linear chains below DP24 are unlikely to form crystallites.

Various types of hydrothermal treatment have been used to reduce starch digestibility. Particularly, autoclaving has been used to increase RS (8–16). The autoclaving-mediated formation of RS can be affected by amylose content (9), treatment time, and use of acid (14), lintnerization (13), and genotypes (12). It was reported that high-pressure autoclaving had an effect similar to that of the treatment in a boiling-water bath in obtaining RS (11). Recently, we found that a combined use of autoclaving and  $\beta$ -amylolysis can be used to reduce the digestibility of normal corn starch and wheat starch (16). In addition, acid treatment has been used to increase the chain mobility of HACS and thus to improve the ordering of linear chains during annealing and heat–moisture treatment (17).

By increasing the content of  $\alpha$ -1,6 glucosidic linkages (i.e., branch density), digestibility can also be reduced (18–20). This methodology is based on the fact that  $\alpha$ -1,6 linkages are much less susceptible to enzymatic hydrolysis than  $\alpha$ -1,4 linkages (21, 22). Recently, we have shown that highly branched malto-oligosaccharides and phytyloglycogen have lower digestibility than normal and waxy corn starches (20).

The present study was a follow-up of our previous work (16). The goal was to advance the  $\beta$ -amylolysis-based strategy for reducing the digestibility of normal corn starch (NCS). We hypothesized that the acid treatment of NCS starch granules can promote amylose crystallization during hydrothermal treatment and enhance the reduction of in vitro digestibility after  $\beta$ -amylolysis. To test the hypothesis, NCS was treated using hydrogen chloride solution and then subjected to autoclaving and  $\beta$ -amylolysis. Starch materials at each stage were analyzed for chain length distribution,

\*Corresponding author [phone (765) 494-6317; fax (765) 494-7953; e-mail yao1@purdue.edu].

amount of ordered structure, crystalline pattern, and in vitro digestibility.

## MATERIALS AND METHODS

**Materials.** NCS and high-amylose starch (HylonVII) were obtained from National Starch and Chemical Co. (Bridgewater, NJ). Pancreatin and amyloglucosidase were purchased from Sigma (St. Louis, MO). Isoamylase, pullulanase, and GOPOD assay kit were purchased from Megazyme (Bray, Ireland).  $\beta$ -Amylase (BBA) was a gift from Genencor (Rochester, NY). The activity of  $\beta$ -amylase was 16400 Betamyl units/mL determined using the Betamyl method (Megazyme).

**Methods.** *Acid Treatment.* NCS (in the form of a 20% slurry) was treated by 1.0% hydrogen chloride at 55 °C. Acid-treated starch slurry was neutralized using 1.0% sodium hydroxide and desalted through repetitive washing using deionized water. Starch cakes were air-dried in the fume hood at room temperature (22 °C), ground using a high-speed blender (Waring Laboratory, Torrington, CT), and passed through an 80 mesh sieve (180  $\mu$ m). The yield of starch was 76.1, 74.7, 78.6, and 65.6% for 2, 5, 10, and 20 h of acid treatment, respectively, based on the mass of native starch. The materials obtained were labeled 2h-AT, 5h-AT, 10h-AT, and 20h-AT for the starch materials subjected to acid treatment (acid treatment abbreviated as AT) for 2, 5, 10, and 20 h, respectively.

*Autoclaving.* The moisture contents of NCS and 2h-AT, 5h-AT, 10h-AT, and 20h-AT starch materials were adjusted to 35% using deionized water. The starch was pressed by hand through a 20 mesh sieve to form a collection of loosely compacted grains. The grains were then subjected to three cycles of autoclaving that comprised 45 min at 121 °C, a 15 min temperature ramp-up, and a 15 min ramp-down. After cooling at room temperature, the material was air-dried and collected, ground using the high-speed blender, and passed through an 80 mesh sieve. The starch solids obtained were labeled NCS-AC (autoclaving abbreviated as AC) for the non-acid-treated material and 2h-AT-AC, 5h-AT-AC, 10h-AT-AC, and 20h-AT-AC, respectively, for the materials prepared from those subjected to 2, 5, 10, and 20 h of acid treatment.

*$\beta$ -Amylolysis.* For each autoclaved starch, a portion was subjected to  $\beta$ -amylolysis. Starch particles were suspended in pH 5.5, 50 mM sodium acetate buffer to form a 20% (w/w) suspension. To this was added  $\beta$ -amylase at 0.50% (w/w) based on starch. The reaction was conducted in a shaking water bath at 55 °C at 70 rpm for 20 h. Thereafter, the reactants were centrifuged at 3000g for 10 min to collect starch precipitates. Each precipitate was washed five times, each time using 3 times by weight of deionized water to remove enzyme and soluble substances. The non-soluble materials were collected and dried in oven at 55 °C, and the solids obtained were ground and passed through an 80 mesh sieve. The yield of collected  $\beta$ -dextrin was 34.2% for non-acid-treated material and 46.7, 49.4, 39.4, and 32.3% for materials that had undergone 2, 5, 10, and 20 h of acid treatment, respectively, based on the mass of corresponding autoclaved starches. The starch materials thus prepared were labeled NCS-AC-BA ( $\beta$ -amylolysis abbreviated as BA) for non-acid-treated material and 2h-AT-AC-BA, 5h-AT-AC-BA, 10h-AT-AC-BA, and 20h-AT-AC-BA, respectively, for those prepared from starch subjected to 2, 5, 10, and 20 h of acid treatment.

*Analysis of Starch Chain Length Distribution.* The chain length distribution of starch was analyzed using high-performance size exclusion chromatography (HPSEC) as described by Hickman et al. (16), with normalization of the chromatogram by the total area from retention time of 10–19 min. For each starch, the chain populations were determined using the minima in the chromatograms. Amylose content of each starch material (except for 20h-AT-AC-BA) was determined from the chromatogram by integrating the area from the 11 min point to the minimum at the right side of the first peak (population 1 for amylose peak, Figure 1). For 20h-AT-AC-BA, population 1 was determined using the same scale as for 10h-AT-AC-BA. The total mass was determined by integrating the area from the 11 min to the 17.5 min point. To determine the branch density, the chromatogram (mass-based) was converted to that of a molar-based using calibration curve (23). The number-average chain length (average CL) was determined by the equation  $CL = \sum(NM)/\sum N$ . The integration region was from 11 to 17.5 min to include the entire area of debranched starch. The branch density was calculated as the inverse of average CL.

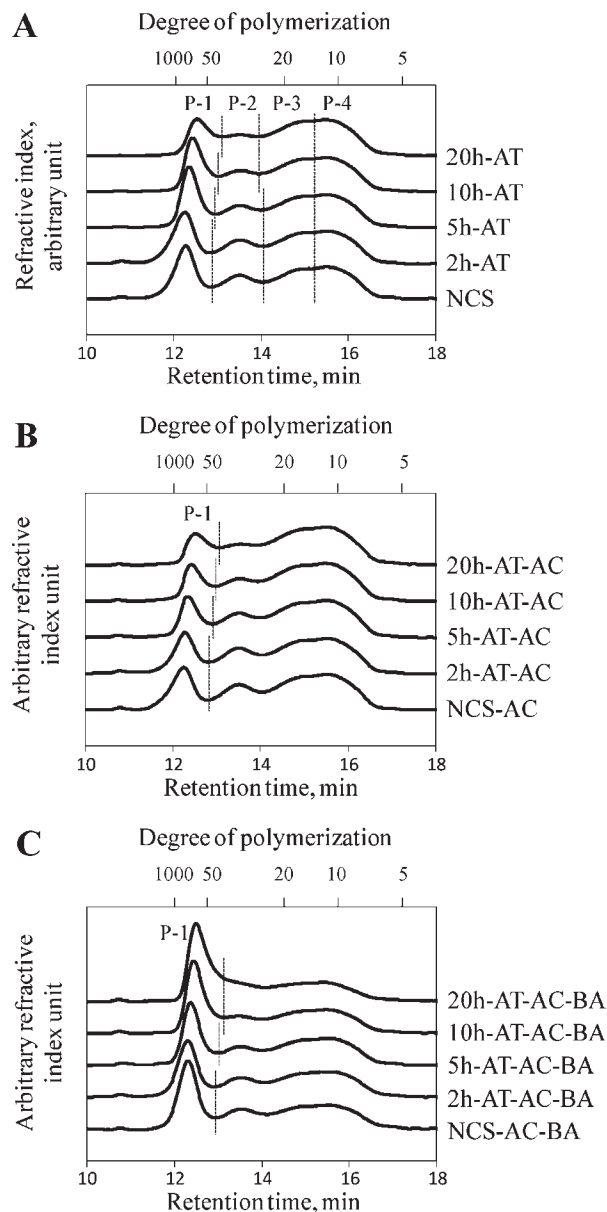


**Figure 1.** Chain length distribution of NCS and starch materials that had undergone acid treatment (A), autoclaving after acid treatment (B), and additional  $\beta$ -amylolysis after autoclaving (C). Populations 1–4 (P-1–P-4) are indicated using dotted lines.

*DSC Analysis.* To evaluate the ordered structure of the prepared starch materials, differential scanning calorimetry (DSC, TA DSC Q2000) was used in a procedure described by Hickman et al. (16) with minor modifications. In a standard TA hermetic aluminum pan, 5.0 mg of starch and deionized water were added to make a 30% solid dispersion. The pan was sealed and allowed to equilibrate for 2 h at room temperature before being loaded. The scans were performed beginning with equilibration at 30 °C and held isothermal for 3 min. The temperature within the DSC unit cell was then raised at 5 °C/min to 120 °C. Data were collected and exported to an Excel spreadsheet. Due to pressure limitations of aluminum pans, only heat flow below 100 °C was reported.

*X-ray Powder Diffraction.* The X-ray powder diffraction analysis was conducted using the procedure described by Hickman et al. (16) with minor modifications. About 500 mg of sample was back-pressed into an aluminum holder and mounted on a Philips PW3710 diffractometer interfaced to a personal computer. The X-ray tube was operated at 40 kV and 25 mA, and Ni-filtered Cu K $\alpha$  radiation ( $\lambda = 1.5418$  Å) was used. The intensity data were collected at room temperature in the  $2\theta$  range 8–38° with a step width of 0.01°, and the time spent at each step was 5 s.

**Table 1.** Percentages of Population 1 (P-1), Branch Density, and Crystallinity and Area of 12.9° Peak of Starch Materials

starch material		P-1 (%) <sup>a</sup>	branch density (%) <sup>a</sup>	crystallinity (%) <sup>b</sup>	12.9° peak area (arbitrary units) <sup>b</sup>
native starch-based	NCS	28.7	4.7	15.1	0.0
	NCS-AC	23.4	5.0	4.1	5.8
	NCS-AC-BA	36.5	4.4	5.6	13.8
2 h acid treatment	2h-AT	28.6	4.7	14.0	0.0
	2h-AT-AC	22.0	5.1	4.6	7.2
	2h-AT-AC-BA	32.1	4.7	4.9	9.1
5 h acid treatment	5h-AT	27.9	4.9	14.7	0.0
	5h-AT-AC	20.0	5.3	9.2	8.6
	5h-AT-AC-BA	32.2	4.7	8.6	12.3
10 h acid treatment	10h-AT	25.8	5.2	16.1	0.0
	10h-AT-AC	18.3	5.6	12.0	10.2
	10h-AT-AC-BA	39.6	4.4	12.2	13.8
20 h acid treatment	20h-AT	21.9	5.6	15.7	0.0
	20h-AT-AC	18.6	5.8	14.0	10.4
	20h-AT-AC-BA	45.7	3.9	12.6	16.5

<sup>a</sup> Calculated from the chromatograms in **Figure 1**. <sup>b</sup> Calculated from the data in **Figure 3**.

The patterns were smoothed for further analysis by the PC-APD (version 3.6) software. Starch crystallinity was determined using the procedure described by Hickman et al. (16). Specifically, the amount of V-type crystallites was evaluated using the area of the 12.9° peak (12.0°–13.8°).

**In Vitro Digestibility.** The in vitro digestibility of starch materials was measured according to the protocol described by Englyst et al. (1) with modifications. All starch suspensions containing added guar gum were heated in a boiling water bath for 10 min. After the suspension had cooled and stabilized in a 37 °C water bath, the enzyme preparation was added. The enzyme preparation contained pancreatin and amyloglucosidase following the Englyst assay protocol (1). After 120 min of reaction, the reactant was aliquoted and mixed with 2 volumes of ethanol. The mixtures were used as the stock solutions for glucose assay using the GOPOD procedure with an assay kit (Megazyme). The amount of glucose produced was used to calculate the portion of glucan converted. Statistical analysis of data was conducted using PROC ANOVA in SAS (version 9.2). The Tukey test was utilized with a significant *F* test ( $P < 0.05$ ).

## RESULTS AND DISCUSSION

**Chain Length Distribution of Starch Materials.** Chain length distributions of NCS and starch materials subjected to acid treatment, additional autoclaving, and additional  $\beta$ -amylolysis after autoclaving are shown in **Figure 1**. The chain length distribution of NCS is consistent with our previous studies, showing a polymodal pattern (16). Four populations are labeled in **Figure 1A**: population 1 for amylose or its residues after acid treatment, population 2 for amylopectin long chains, population 3 for most short B chains, and population 4 for most A chains. After acid treatment, the most pronounced changes were in the molecular weight and amount of population 1, suggesting the impact of acid-catalyzed hydrolysis on amylose molecules. The change caused by 2 h of acid treatment was negligible, whereas 5, 10, and 20 h of treatment led to stepwise reduction of amylose molecular weight. After 10 and 20 h, the amount of population 1 was reduced to 25.8 and 21.9%, respectively, from 28.7% of nontreated NCS (**Table 1**). It is believed that the reduction was related to the release of short linear segments from amylose. In chromatograms, the released short linear segments can be embedded within the chain populations of debranched amylopectin. In addition, some materials released after acid treatment could be removed during the extraction of residual starches, which could also contribute to a reduction of population 1.

Chain length distributions of starch materials subjected to autoclaving are shown in **Figure 1B**. Autoclaving did not change the general pattern that higher levels of acid treatment correlated with lower amounts of population 1. However, a comparison of panels **A** and **B** of **Figure 1** shows that autoclaving reduced the amount of population 1 for both native NCS and acid-treated starch materials. For example, after autoclaving, population 1 was reduced from 28.7 to 23.4% for NCS, from 27.9 to 20.0% for 5h-AT, and from 21.9 to 18.6% for 20h-AT (**Table 1**). Such a reduction indicates that autoclaving can lead to substantial degradation of amylose molecules. A similar outcome was observed in our previous study (16).

By trimming the external chains of amylopectin and amylose molecules,  $\beta$ -amylolysis substantially changed the chain length distribution (**Figure 1C**). One important outcome was that population 1 increased drastically. For example, for NCS-based material,  $\beta$ -amylolysis improved the amount of population 1 from 23.4 to 36.5%. For 10h-AT-based material, population 1 increased from 18.3 to 39.6% (**Table 1**). Particularly, after  $\beta$ -amylolysis, the increase of population 1 was much higher for starch materials that had undergone higher levels of acid treatment. For example, for the 2 h acid-treated starch,  $\beta$ -amylolysis increased population 1 from 22.0 to 32.1%. In contrast, for 20 h acid-treated starch,  $\beta$ -amylolysis increased population 1 from 18.6 to 45.7%.

The large increase of population 1 can be attributed to two factors. The first factor is related to a preferential  $\beta$ -amylolysis of amylopectin over amylose.  $\beta$ -Amylase removes maltosyl units from the nonreducing ends of glucan chains, and the hydrolysis rate should be much higher for branched molecules (amylopectin) than for linear molecules (amylose). For acid-treated starch, the hydrolysis at the amorphous regions of amylopectin may create additional nonreducing ends, thus increasing the extent of  $\beta$ -amylolysis of branched materials. The second factor is related to the water-washing procedure for extracting  $\beta$ -dextrin. The washing procedure removed a large portion of branched materials, and the quantity of removed material could be increased by elevated levels of acid treatment. Overall, both factors led to substantially increased population 1 after  $\beta$ -amylolysis.

**Table 1** shows the branch density (reverse of number-average CL) of starch materials that have undergone acid treatment, autoclaving, and  $\beta$ -amylolysis. In general, acid treatment slightly



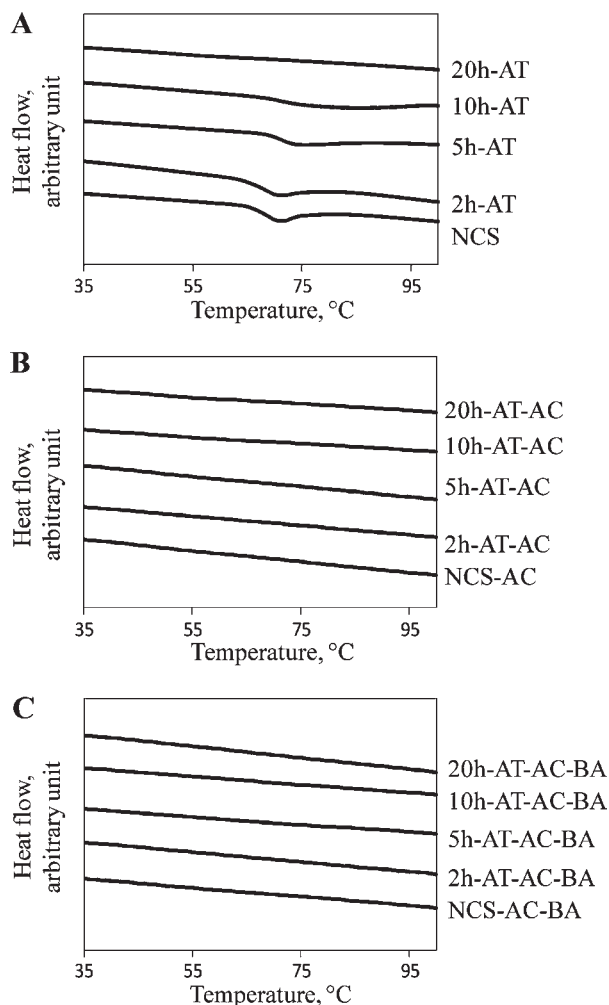


**Figure 2.** DSC heat flow of NCS and starch materials that had undergone acid treatment (A), autoclaving after acid treatment (B), and additional  $\beta$ -amylolysis after autoclaving (C).

increased the calculated branch density due to the reduced chain length. Autoclaving had a similar effect, which was also associated with molecular degradation. In contrast,  $\beta$ -amylolysis led to a minor reduction of branch density at a low level of acid treatment (e.g., for 2 h of treatment) and a large reduction at a high level of acid treatment (e.g., for 20 h of treatment). In general, the reduction of branch density was associated with the increase of population 1.

**Thermal Behavior of Starch Materials.** Figure 2 shows the DSC heat flow profiles of starch materials in the temperature range of 35–100 °C. Due to pressure limitations of DSC pans, higher temperatures led to leaking. Nevertheless, some important information was obtained, especially by comparing the results of DSC and X-ray powder diffraction (discussed later). Figure 2A shows the impact of acid treatment on starch gelatinization. An evident phenomenon was that acid treatment substantially increased the gelatinization temperature. For NCS, the peak gelatinization temperature was 71 °C. Two hours of acid treatment had negligible influence on the peak temperature, corresponding to its negligible impact on starch chain length distribution (Figure 1A). In contrast, 5 h of acid treatment increased the peak temperature to about 76 °C with a widened peak. The effect of 10 h of acid treatment was more pronounced, generating a much flattened peak in the range of 66–95 °C with the peak at about 82 °C. For the starch subjected to 20 h of acid treatment, the enthalpy change was undetectable below 100 °C.

Panels B and C of Figure 2 illustrate the thermal behaviors of starch materials that had undergone autoclaving and  $\beta$ -amylolysis. The heat flow curves were all straight, showing undetectable enthalpy change below 100 °C. Therefore, it is concluded that for each starch material there is no ordered structure that can be melted below 100 °C.

**Crystalline Structure of Starch Materials.** The effect of acid treatment on the structural arrangement of NCS is shown in Figure 3A. All of the X-ray powder diffraction patterns display peaks around 10.0°, 11.2°, 15.2°, 17.1°, 18.0°, 19.9°, 23.0°, 26.5°, 28.9°, and 30.3° of  $2\theta$ . These profiles are characteristic of A-type starch diffraction (24). The crystallinity of NCS was 15.1% and had been maintained in the range of 14.0–16.1% (Table 1) for all of the treated samples. Considering the starch yield of 65.6–78.6% after acid treatment, most of the A-type crystallites were retained through acid treatment. This observation is in congruence with the fact that acid-catalyzed hydrolysis preferentially occurs in the amorphous regions, that is, amylose and amorphous lamellae of amylopectin. As shown in DSC heat flow profiles (Figure 2A), the 2 h acid treatment led to negligible change of endothermic behavior compared to non-acid treatment. The endothermic heat flow occurred at higher temperature range with 5 and 10 h acid treatments and was even undetectable below 100 °C with 20 h of treatment. This clearly indicates that higher levels of acid treatment (at 55 °C) led to increased thermal resistance of A-type crystallites, possibly by an annealing-like process occurring at 55 °C.

Figure 3B shows the effect of autoclaving (121 °C, 35% moisture) on the crystalline pattern of NCS and acid-treated starch materials. For NCS-AC, all A-type crystallites were destroyed. However, concomitant development of 12.9° and 19.7° reflections for V-type crystallites resulted in 4.1% crystallinity (Table 1). For 2h-AT-AC, most A-type crystallites were removed, but the amount of V-type crystallites was higher than that of NCS-AC, demonstrated by an increase of 12.9° peak area from 5.8 to 7.2 (Table 1). Retention of A-type crystallites was evidenced with 5h-AT-AC (crystallinity of 9.2%) with elevated levels of V-type crystallites (12.9° peak area of 8.6). Larger amounts of A-type crystallites were preserved for 10h-AT-AC and 20h-AT-AC with higher amounts of V-type (12.9° peak areas of 10.2 and 10.4, respectively), resulting in crystallinities of 12.0 and 14.0%, respectively. The appearance of V-type crystallites clearly indicates the molecular mobility of amylose chains during autoclaving. Higher levels of acid treatment substantially reduced amylose molecular weight (Figure 1A), which in turn facilitated the migration of linear segments and formation of V-type crystallites. Overall, it can be concluded that the acid treatment has two seminal effects on starch materials undergoing the autoclaving procedure: (1) increased mobility of amylose leading to V-type crystallites and (2) enhanced thermal resistance of A-type crystalline structure.

Comparison of panels B and C of Figure 3 shows that the general crystalline pattern (containing both A- and V-type crystallites) was not changed by  $\beta$ -amylolysis. Table 1 also shows that  $\beta$ -amylolysis did not substantially change the crystallinity values. However, the amount of V-type crystallites was increased due to  $\beta$ -amylolysis. For example, for NCS-based starch materials and the materials subjected to 20 h of acid treatment, the 12.9° peak areas increased from 5.8 to 13.8 and from 10.4 to 16.5, respectively. Considering the yield of  $\beta$ -dextrin (32–50%), it is possible that A-type crystallites were more easily removed than V-type crystallites during the extraction process, leading to an enrichment of V-type crystallites in the  $\beta$ -dextrins collected. Conceivably, V-type crystallites, which mostly contain amylose and its residues, were much less soluble or dispersible than A-type crystallites that mostly contain amylopectin.

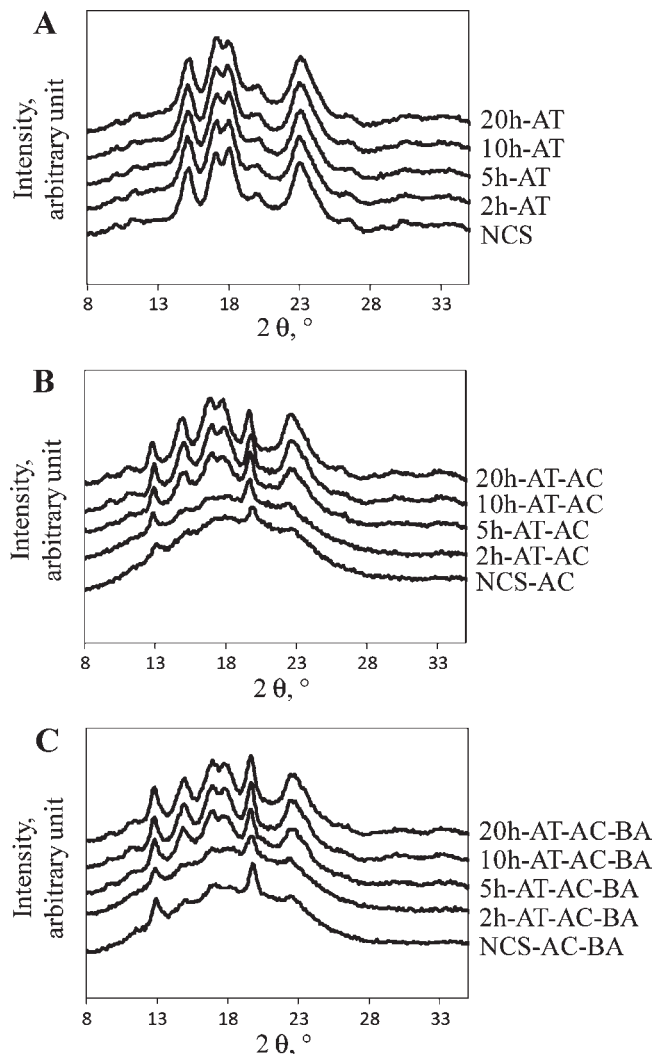


**Figure 3.** X-ray powder diffraction patterns of NCS and starch materials that had undergone acid treatment (A), autoclaving after acid treatment (B), and additional  $\beta$ -amylolysis after autoclaving (C).

**In Vitro Digestibility.** Figure 4 shows the digestibility of starch materials denoted by the portion of glucan converted to glucose. The Englyst assay was used due to its correlation with a human study (1) for the reference to actual digestion behaviors. In our study, HACS was used as a reference to compare the digestibility of all NCS-originated starch materials.

An overview of Figure 4 indicates that acid treatment, autoclaving, and  $\beta$ -amylolysis were factors contributing to reduced digestibility. Among them,  $\beta$ -amylolysis appears to be the most effective one, particularly with starch materials subjected to high levels of acid treatment. For example, the portions of converted glucan for 10h-AT-AC-BA and 20h-AT-AC-BA were 0.643 and 0.587, respectively, less than that of HACS (0.690). For those with non-acid treatment or low levels of treatment (2 or 5 h), the effect of  $\beta$ -amylolysis was not as drastic as those with high levels of acid treatment (10 or 20 h), suggesting a synergistic effect between acid treatment and  $\beta$ -amylolysis on the reduction of starch digestibility.

In our previous paper (16), the “fringed micelle” model was used to describe the microstructure of starch materials that have undergone autoclaving and  $\beta$ -amylolysis. These materials contain organized regions with ordered linear segments of amylose and amylopectin as well as amorphous regions with nonassociated amylose segments and amylopectin branch areas and short

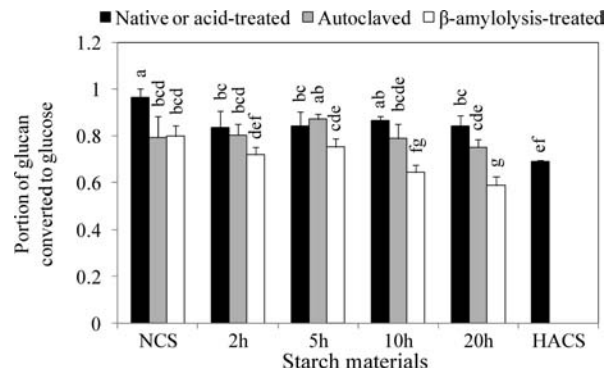


**Figure 4.** Starch digestibility evaluated using the portion of glucan converted to glucose after 120 min of enzyme reaction. The X-axis indicates individual groups originated from non-acid-treated NCS and from starches subjected to 2, 5, 10, or 20 h of acid treatment. There are three samples for each group: (1) native NCS or starch subjected to acid treatment (indicated as “Native or acid-treated”); (2) the one with additional autoclaving (indicated as “Autoclaved”); and (3) the one with additional autoclaving followed by  $\beta$ -amylolysis (indicated as “ $\beta$ -amylolysis-treated”). Native HACS is used as a reference. For each sample, the mean value (column height) and standard deviation (error bar) ( $n \geq 4$ ) are shown. Significant differences are denoted by different letters ( $p < 0.05$ ).

chains. The digestibility of starch is governed by the amount of resistant crystallites in organized regions and the amount of  $\alpha$ -1,6 glucosidic linkages in the amorphous regions.

In the current study, the application of acid treatment had substantial effects on the outcome of autoclaving and  $\beta$ -amylolysis and, therefore, the digestibility of the final preparations. Two structure-ordering events associated with acid treatment should be considered to address starch digestibility: (1) generation of thermally resistant A-type crystallites right after acid treatment and (2) drastic enrichment of amylose-based linear molecules after  $\beta$ -amylolysis.

In general, high levels of acid treatment at 55 °C substantially increased the thermal stability of A-type crystallites against autoclaving and  $\beta$ -amylolysis (Figure 3B,C). However, the retained A-type crystallites had limited roles in reducing digestibility. After autoclaving, starch materials subjected to 5, 10, and 20 h of acid treatment all retained significant amounts of A-type crystallites (Figure 3B). However, none of them showed appreciable digestibility reduction compared with starch materials retaining negligible amounts of A-type crystallites (NCS-AT and 2h-AT-AC).

In contrast, an enrichment of linear molecules after  $\beta$ -amylolysis seems to be a major factor for reduced digestibility. This was particularly the case for starch materials subjected to longer durations of acid treatment. For 10h-AT-AC-BA and 20h-AT-AC-BA, population 1 increased from 18.3 to 39.6% and from 18.6 to 45.7% due to  $\beta$ -amylolysis (Table 1), which correlated to reductions of converted glucan from 0.788 to 0.643 and from 0.751 to 0.587, respectively (Figure 4).

In summary, the present study shows that acid treatment substantially increased the thermal resistance of A-type crystallites of NCS and promoted the development of V-type crystallites after autoclaving. After  $\beta$ -amylolysis, both A- and V-type crystallites were preserved. Particularly, release of maltose and partial removal of branched glucans during the extraction of  $\beta$ -dextrins enriched linear glucans, leading to reduced digestibility. From the perspective of industrial application, one may consider that the strategy proposed in this work is to reduce starch digestibility by “enriching amylose”, which is more cost-effective than

conventional amylose fractionation strategies such as amylose leaching and solvent extraction.

#### LITERATURE CITED

- (1) Englyst, H.; Kingman, S.; Cummings, J. Classification and measurement of nutritionally important starch fractions. *Eur. J. Clin. Nutr.* **1992**, *46* (Suppl. 2), 33–50.
- (2) Thompson, D. Strategies for the manufacture of resistant starch. *Trends Food Sci. Technol.* **2000**, *11*, 245–253.
- (3) Guraya, H. S.; James, C.; Champagne, E. T. Effect of enzyme concentration and storage temperature on the formation of slowly digestible starch from cooked debranched rice starch. *Starch/Staerke* **2001**, *53*, 131–139.
- (4) Guraya, H. S.; James, C.; Champagne, E. T. Effect of cooling and freezing on the digestibility of debranched rice starch and physical properties of the resulting material. *Starch/Staerke* **2001**, *53*, 64–74.
- (5) Shin, S. I.; Choi, H. J.; Chung, K. M.; Hamaker, B. R.; Park, K. H.; Moon, T. W. Slowly digestible starch from debranched waxy sorghum starch: preparation and properties. *Cereal Chem.* **2004**, *81*, 404–408.
- (6) Gidley, M. J.; Bulpin, P. V. Crystallization of maltooligosaccharides as models of the crystalline forms of starch – minimum chain-length requirement for the formation of double helices. *Carbohydr. Res.* **1987**, *161*, 291–300.
- (7) Eerlingen, R. C.; Deceuninck, M.; Delcour, J. A. Enzyme-resistant starch. 2. Influence of amylose chain-length on resistant starch formation. *Cereal Chem.* **1993**, *70*, 345–350.
- (8) Nyman, M.; Pedersen, B.; Siljestrom, M.; Asp, N.; Eggum, B. Formation of enzyme resistant starch during autoclaving of wheat-starch: studies in vitro and in vivo. *J. Cereal Sci.* **1987**, *6*, 159–172.
- (9) Escarpa, A.; Gonzalez, M.; Manas, E.; Garcia-Diz, L.; Saura-Calixto, F. Resistant starch formation: standardization of a high-pressure autoclave process. *J. Agric. Food Chem.* **1996**, *44*, 924–928.
- (10) Skrabanja, V.; Kreft, I. Resistant starch formation following autoclaving of buckwheat (*Fagopyrum esculentum* Moench) groats. An in vitro study. *J. Agric. Food Chem.* **1998**, *46*, 2020–2023.
- (11) Garcia-Alonso, A.; Jimenez-Escrig, A.; Martin-Carron, N.; Bravo, L.; Saura-Calixto, F. Assessment of some parameters involved in the gelatinization and retrogradation of starch. *Food Chem.* **1999**, *66*, 181–187.
- (12) Skrabanja, V.; Liljeberg, H.; Hedley, C.; Kreft, I.; Bjorck, I. Influence of genotype and processing on the in vitro rate of starch hydrolysis and resistant starch formation in peas (*Pisum sativum* L.). *J. Agric. Food Chem.* **1999**, *47*, 2033–2039.
- (13) Aparicio-Saguilan, A.; Flores-Huicochea, E.; Tovar, J.; Garcia-Suarez, F.; Gutierrez-Meraz, F.; Bello-Perez, L. A. Resistant starch-rich powders prepared by autoclaving of native and lintnerized banana starch: partial characterization. *Starch/Staerke* **2005**, *57*, 405–412.
- (14) Onyango, C.; Bley, T.; Jacob, A.; Henle, T.; Rohm, H. Influence of incubation temperature and time on resistant starch type III formation from autoclaved and acid-hydrolysed cassava starch. *Carbohydr. Polym.* **2006**, *66*, 494–499.
- (15) Gonzalez-Soto, R.; Mora-Escobedo, R.; Hernandez-Sanchez, H.; Sanchez-Rivera, M.; Bello-Perez, L. The influence of time and storage temperature on resistant starch formation from autoclaved debranched banana starch. *Food Res. Int.* **2007**, *40*, 304–310.
- (16) Hickman, B. E.; Janaswamy, S.; Yao, Y. Autoclave and  $\beta$ -amylolysis lead to reduced in vitro digestibility of starch. *J. Agric. Food Chem.* **2009**, *57*, 7005–7012.
- (17) Brumovsky, J. O.; Thompson, D. B. Production of boiling-stable granular resistant starch by partial acid hydrolysis and hydrothermal treatments of high-amylose maize starch. *Cereal Chem.* **2001**, *78*, 680–689.
- (18) Lee, C.; Le, Q.; Kim, Y.; Shim, J.; Lee, S.; Park, J.; Lee, K.; Song, S.; Auh, J.; Lee, S.; Park, K. Enzymatic synthesis and properties of highly branched rice starch amylose and amylopectin cluster. *J. Agric. Food Chem.* **2008**, *56*, 126–131.
- (19) Ao, Z.; Simsek, S.; Zhang, G.; Venkatachalam, M.; Reuhs, B.; Hamaker, B. Starch with a slow digestion property produced by altering its chain length, branch density, and crystalline structure. *J. Agric. Food Chem.* **2007**, *55*, 4540–4547.
- (20) Shin, J.; Simsek, S.; Reuhs, B.; Yao, Y. Glucose release of water-soluble starch-related  $\alpha$ -glucans by pancreatin and amyloglucosidase is affected by the abundance of  $\alpha$ -1,6-glycosidic linkages. *J. Agric. Food Chem.* **2008**, *56*, 10879–10886.
- (21) Pazur, J.; Ando, T. The hydrolysis of glucosyl oligosaccharides with  $\alpha$ -D-(1,4) and  $\alpha$ -D-(1,6) bonds by fungal amyloglucosidase. *J. Biol. Chem.* **1960**, *235*, 297–302.
- (22) Pazur, J.; Kleppe, K. The hydrolysis of  $\alpha$ -D-glucosides by amyloglucosidase from *Aspergillus niger*. *J. Biol. Chem.* **1962**, *237*, 1002–1006.
- (23) Yao, Y.; Thompson, D.; Guiltinan, M. Maize starch branching enzyme (SBE) isoforms and amylopectin structure: in the absence of SBEIIb, the further absence of SBEIa leads to increased branching. *Plant Physiol.* **2004**, *136*, 515–523.
- (24) Cairns, P.; Bogracheva, T.; Ring, S.; Hedley, C.; Morris, V. Determination of the polymorphic composition of smooth pea starch. *Carbohydr. Polym.* **1997**, *32*, 275–282.

---

Received for review March 27, 2010. Revised manuscript received June 20, 2010. Accepted June 28, 2010.